Denitrification in marine sediments: A model study

Jack J. Middelburg, Karline Soetaert, Peter M. J. Herman, and Carlo H. R. Heip

Centre for Estuarine and Coastal Ecology, Netherlands Institute of Ecology, Yerseke

Abstract. The rate and factors controlling denitrification in marine sediments have been investigated using a prognostic diagenetic model. The model is forced with observed carbon fluxes, bioturbation and sedimentation rates, and bottom water conditions. It can reproduce rates of aerobic mineralization, denitrification, and fluxes of oxygen, nitrate, and ammonium. The globally integrated rate of denitrification is estimated by this model to be about 230-285 Tg N yr^{-1}, with about 100 Tg N yr^{-1} occurring in shelf sediments. This estimate is significantly higher than literature estimates (12-89 Tg N yr^{-1}), mainly because of a proposed upward revision of denitrification rates in slope and deep-sea sediments. Higher sedimentary denitrification estimates require a revision of the marine nitrogen budget and lowering of the oceanic residence time of nitrogen down to about 2×10^3 years and are consistent with reported low N/P remineralization ratios between 1000 and 3000 m. Rates of benthic denitrification are most sensitive to the flux of labile organic carbon arriving at the sediment-water interface and bottom water concentrations of nitrate and oxygen. Denitrification always increases when bottom water nitrate increases but may increase or decrease if oxygen in the bottom water increases. Nitrification is by far the most important source of nitrate for denitrification, except for organic-rich sediments underlying oxygen-poor and nitrate-rich water.

1. Introduction

Ice core bubble data convincingly demonstrate that atmospheric carbon dioxide concentration during interglacial times was about 280 parts per million by volume (ppmv) but was less than about 200 ppmv during glacial times [*Barnola et al.*, 1987]. This change reflects adjustments in the distribution of carbon between the ocean, atmosphere, and biosphere. The ocean is the only carbon reservoir that is large enough, yet sufficiently dynamic, to cause such changes in atmospheric carbon dioxide concentrations [*Broecker*, 1982]. Changes in the oceanic carbon cycle have been attributed to changes in oceanic nutrient inventories, ocean alkalinity, ocean circulation, and biological activity, but the mechanisms involved remain unclear.

Photosynthesis in oceanic surface waters results in a downward flux of detrital carbon which, after respiration, causes enhanced concentrations of carbon dioxide in deeper water. This biological pump maintains a disequilibrium in CO_2 concentrations between the upper ocean-atmosphere-biosphere on the one hand and the deep ocean on the other hand. The efficiency of the biological pump depends mainly on the supply of nutrients, in particular, phosphate and nitrate, to the illuminated surface layer. Depending on the timescale considered, phosphorus or nitrogen may be the limiting macronutrient for life in the ocean. The oceanic residence time of phosphorus (2×10^4 - 10^5 years [*Van Cappellen and Ingall*, 1994]) is long relative to the renewal time of ocean deep waters (10^3 years). As a consequence, oceanic P inventories can only change over long timescales ($> 5 \times 10^4$ years [*Shaffer*, 1989]).

Nitrogen appears to be the main factor limiting productivity in the ocean today [*Fanning*, 1992] and has a much shorter residence time (of the order of 10^3 to 10^4 years) indicating that fluctuations in its inventory on glacial-interglacial timescales are likely [*McElroy*, 1983]. Such changes in nitrogen inventories could affect the efficiency of the biological pump and thus levels of atmospheric carbon dioxide.

Recent studies have gathered evidence for low denitrification rates and a consequent increase in the oceanic nitrogen inventory during glacial periods. On the basis of $^{15}N/^{14}N$ ratios, *Shäfer and Ittekkot* [1993], *Altabet et al.* [1995], and *Ganeshram et al.* [1995] have argued that water column denitrification was lower during glacial periods. Studies by *Berger and Keir* [1984], *Christensen et al.* [1987], *Shaffer* [1990], and *Christensen* [1994] indicate that global sedimentary denitrification during glaciation may have been lowered because of the reduced area of continental shelves, where most of the sedimentary denitrification is thought to occur.

The present-day oceanic nitrogen budget seems to be unbalanced because the supply of nitrogen to the ocean is much smaller than its removal rate [*McElroy*, 1983; *Codispoti*, 1995]. Present-day sinks of nitrogen include burial in sediments (10-27 Tg N yr^{-1} [*Codispoti and Christensen*, 1985; *Christensen*, 1994; *Wollast*, 1991]), organic nitrogen exports (13-16 Tg N yr^{-1} [*Codispoti and Christensen*, 1985; *Galloway et al.*, 1995]), denitrification in the water column (60-90 Tg N yr^{-1} [*Codispoti and Christensen*, 1985; *Devol*, 1991; *Ganeshram et al.*,1995]), and sedimentary denitrification (12-89 Tg N yr^{-1} [*Liu and Kaplan*, 1984; *Codispoti and Christensen*, 1985; *Devol*, 1991; *Christensen*, 1994]). This range in estimates for global sedimentary denitrification must be narrowed before we can understand, quantify, or model excursions in the oceanic nitrogen inventory. The wide range in estimates is inherited

from the very few individual observations that have been used in the upscaling procedures.

In this paper we will use our prognostic numerical diagenetic model for early diagenetic processes from the shelf to abyssal depths [*Soetaert et al.,* 1996a] with the following purposes: (1) to better constrain the global rate of sedimentary denitrification, (2) to reveal the most important factors controlling sedimentary denitrification, and (3) to evaluate the response of sedimentary denitrification to changing oceanographic conditions.

2. Model

2.1. Model Description

The diagenetic model used in this study is an updated, steady state version of the numerical model of *Soetaert et al.* [1996a]. This model has been developed to examine the sedimentary cycling of carbon, nitrogen, and oxygen from shelf to abyssal depths and to allow coupling with water column models that describe biogeochemical cycles of carbon, nitrogen, and oxygen. Although it is possible to accurately reproduce measured concentration versus depth profiles in sediments [*Soetaert et al.,* 1996b], the primary aim is to reproduce sediment-water fluxes along sedimentary gradients.

The diagenetic model is based on the general diagenetic equations of *Berner* [1980]. Particles are transported by advection (sediment deposition), by compaction (induced by porosity gradients), and by the activity of organisms (bioturbation). Bioturbation is included not only as a diffusion-like process but also as a nonlocal exchange process [*Boudreau,* 1986]. Recently, *Soetaert et al.* [1996c] have presented a set of ^{210}Pb data and nonlocal exchange/bioturbation models that allowed them to partition diffusive mixing from nonlocal exchange. They observed that on average 46% (14% to 87%) of the carbon flux arriving at the sediment is injected at some depth in the sediment (4.3 ± 2.7 cm), rather than being included into the sediment by diffusive mixing and sediment accumulation. Moreover, they also reported a regression between the fraction of organic matter (*f*) that is nonlocally exchanged and water depth:

$f =$ 1.58-0.16 × ln(water depth)

though the coefficient of determination is moderate (r^2 = 0.34). The effects of nonlocal mixing on diagenesis will be restricted to the sensitivity analysis because there still are very limited data on nonlocal exchange rates.

Dissolved substances are transported by molecular diffusion which at shallow water depth is enhanced by irrigation in the upper 10 cm. Although a nonlocal solute exchange approach is preferred on theoretical arguments [*Boudreau,* 1984], an enhanced diffusion approach is chosen because data are available [*Archer and Devol,* 1992; *Devol and Christensen,* 1993] and the integrated rates (i.e., sediment-water fluxes) do not depend significantly on the approach chosen.

The complexity of biogeochemical cycles within sediments and our limited understanding of many of these processes require some simplifications to be made. The model explicitly resolves the depth distribution of solid-phase organic carbon and nitrogen, and pore water oxygen, nitrate, and ammonium, while dissolved intermediates (e.g., nitrite, nitrous oxide, and hydroxylamine) and dissolved organic carbon and nitrogen components are neglected. Reduced manganese, iron, and sulphur are lumped together into oxygen demand units (*ODU*) [*Soetaert et al.,* 1996a]. As their names implies, *ODU*s are oxidized when in contact with oxygen. They are subject to the transport of dissolved substances. Because of the lumping of reoxidation of reduced manganese, iron, and sulphur, we do not explicitly model the complex interactions between the carbon, manganese, iron, and sulphur cycles, yet we have included their small effect on the oxygen distribution.

Organic carbon decomposition occurs through the consumption of oxygen (aerobic mineralization) and nitrate (denitrification) and occurs anaerobically. To represent the decrease in organic matter lability with time and depth (in the water column and in the sediment), organic matter degradation is described using two degradable fractions [*Westrich and Berner,* 1984] with fixed first-order rate constants (26 and 0.26 $year^{-1}$) and with different C/N ratios (6.6 and 7.5). Oxygen is consumed by aerobic mineralization and oxidation of ammonium (nitrification) and other reduced substances (*ODU*). Ammonium is liberated by decomposing organic matter, exchanges with the sediment matrix, and is consumed by nitrification and reaction with nitrate. Nitrate is produced by nitrification and consumed by denitrification and nitrate reduction coupled to ammonium oxidation. Hyperbolic functions are used to express the dependence of metabolic activities on oxidant availability and inhibition by other substances. Oxygen consuming processes (aerobic degradation, nitrification, and reoxidation of reduced substances) are limited by oxygen, while nitrate-consuming processes (denitrification and nitrate reduction coupled to ammonium oxidation) are limited by nitrate and inhibited by oxygen. Nitrate consumption linked to the oxidation of ammonium [*Bender et al.,* 1989] will only be considered in sensitivity runs since there is as yet little conclusive evidence for its importance.

2.2. Calibration and Forcing

The model parameters (Table 1) can be grouped into four categories.

The first group of parameters are constant at a global scale and based on *Soetaert et al.* [1996a]. This group includes the stoichiometric coefficients, the dimensionless ammonium sorption coefficient, the porosity and its gradient with depth in sediments, and the parameters of the hyperbolic functions (maximum rates and half-saturation constants). This group also includes those which depend on temperature only, that is, the molecular diffusion coefficients.

The second group includes those transport parameters which are parametrized as a function of water depth [*Soetaert et al.,* 1996a, c; *Middelburg et al.,* 1996], namely, sediment accumulation rate, bioturbation coefficients, irrigation enhancement factors, and nonlocal exchange parameters.

The third group relates to the bottom water conditions (oxygen, nitrate, ammonium, and temperature) which depend on water depth and ocean basin. Bottom water conditions are obtained from composite profiles based on Geochemical Ocean Sections Study (GEOSECS) data: station 17 for the Arctic Ocean, stations 37, 58, 83, 102, 110, 115, and 121 for the Atlantic Ocean, stations 417, 424, 429, 435, 445, and 452 for the Indian Ocean, and stations 201, 217, 224, 242, 273, 286, 322, and 337 for the Pacific Ocean.

Table 1. A Selection of Model Parameters Based on Work by *Soetaert et al.* [1996a, b, c] and *Middelburg et al.* [1996]

Name	Units	Parameters constant at a global scale	
		Value	Description
KsO_2	μM	3	half-saturation constant for O_2 limitation in oxic mineralization
$KsNO_3$	μM	30	half-saturation constant for NO_3 limitation in denitrification
Kin_{O2}^{Denit}	μM	10	half-saturation constant for O_2 inhibition in denitrification
$Kin_{NO3}^{AnoxMin}$	μM	5	half-saturation constant for NO_3 inhibition in anoxic mineralization
$Kin_{O2}^{AnoxMin}$	μM	5	half-saturation constant for O_2 inhibition in anoxic mineralization
Ks_{Nitrif}	μM	1	half-saturation constant for O_2 limitation in nitrification
Ks_{ODUox}	μM	1	half-saturation constant for O_2 limitation in oxidation of ODU
R_{ODUox}	d^{-1}	20	maximum oxidation rate of oxygen demand units
R_{Nitrif}	d^{-1}	20	maximum nitrification rate
γ_{TOC}^{ODU}		1	mol ODU formed per mol C in anoxic mineralization
γ_{TOC}^{O2}		1	mol O_2 used per mol C in oxic mineralization
γ_{TOC}^{NO3}		0.8	mol NO_3 used per mol C in denitrification
γ_{TOC1}^{N}		0.1509	N:C ratio of fast decay detritus
γ_{TOC2}^{N}		0.1333	N:C ratio of slow decay detritus
γ_{NH3}^{O2}		2	mol O_2 needed to oxidize 1 mol of NH_3 in nitrification
NH_3ads		1.3	adsorption coefficient of ammonium
Φ_0		0.95	porosity at the sediment-water interface
ϕ_∞		0.8	porosity at infinite sediment depth
$Coeff_\phi$	cm	4	coefficient for exponential prorosity change
x_b	cm	5	depth below which bioturbation decreases exponentially
$coeff_{Db}$	cm	1	coefficient for exponential bioturbation decrease

Parameters Depending on Water Depth z (m)

Function			
$\omega = 3.3 \times 10^{(-0.8748-0.000435 \times z)}$	cm yr^{-1}		Sediment accumulation rate
$D_b = 4.4 \times 10^{(0.7624-0.000397 \times z)}$	cm^2 yr^{-1}		Diffusive bioturbation rate
Irrigation $= 15.9 \times z^{-0.43}$			Diffusion enhancement factor
$F_c = 1.8 \times 10^{(-0.5086-0.000389 \times z)}$	mmol cm^{-2} yr^{-1}		Flux of labile carbon

Parameters in group four relate to the flux and reactivity of organic matter. The total flux of labile organic matter is a function of water depth [*Middelburg et al.,* 1996], while the reactivity depends on the water depth and temperature distribution in the overlying water column [*Soetaert et al.,* 1996a].

3. Results

3.1. Comparison of Model Results With Literature Data

Model results on aerobic degradation, denitrification, and fluxes of oxygen, nitrate, and ammonium are compared with biogeochemical data extracted from a literature database available at the Netherlands Institute of Ecology [*Middelburg et al.,* 1996]. Figure 1 shows that major trends in the depth distributions are well reproduced given the simplicity of the model, the variability in available data, and our use of globally averaged parameters. Rates of aerobic mineralization (Figure 1b) and ammonium effluxes (Figure 1e), in particular, are well

predicted. Oxygen fluxes (Figure 1d), though within the envelope of data, seem to be somewhat overestimated in upper slope sediments and underestimated in deep-sea sediments. These deviations are largely a consequence of our forcing of total mineralization rates with an imposed exponential relationship between the flux of labile organic carbon and water depth (Figure 1a).

Predicted rates of denitrification (Figure 1c) and the direction of nitrate fluxes (Figure 1f) in sediments in the upper 1000 m of the Pacific Ocean deviate somewhat from those actually observed. These inconsistensies point to the limitations of using globally averaged model parameters and bottom water conditions to reproduce actual observed data. By changing some model parameters, it is possible to obtain model-predicted rates that better fit the actual data. For instance, the discrepancy between model-predicted and observed rates in the Pacific Ocean is reduced significantly by choosing bottom water conditions more like those found in the eastern Pacific (100 μM oxygen and 30 μM nitrate) and doubling the flux of labile
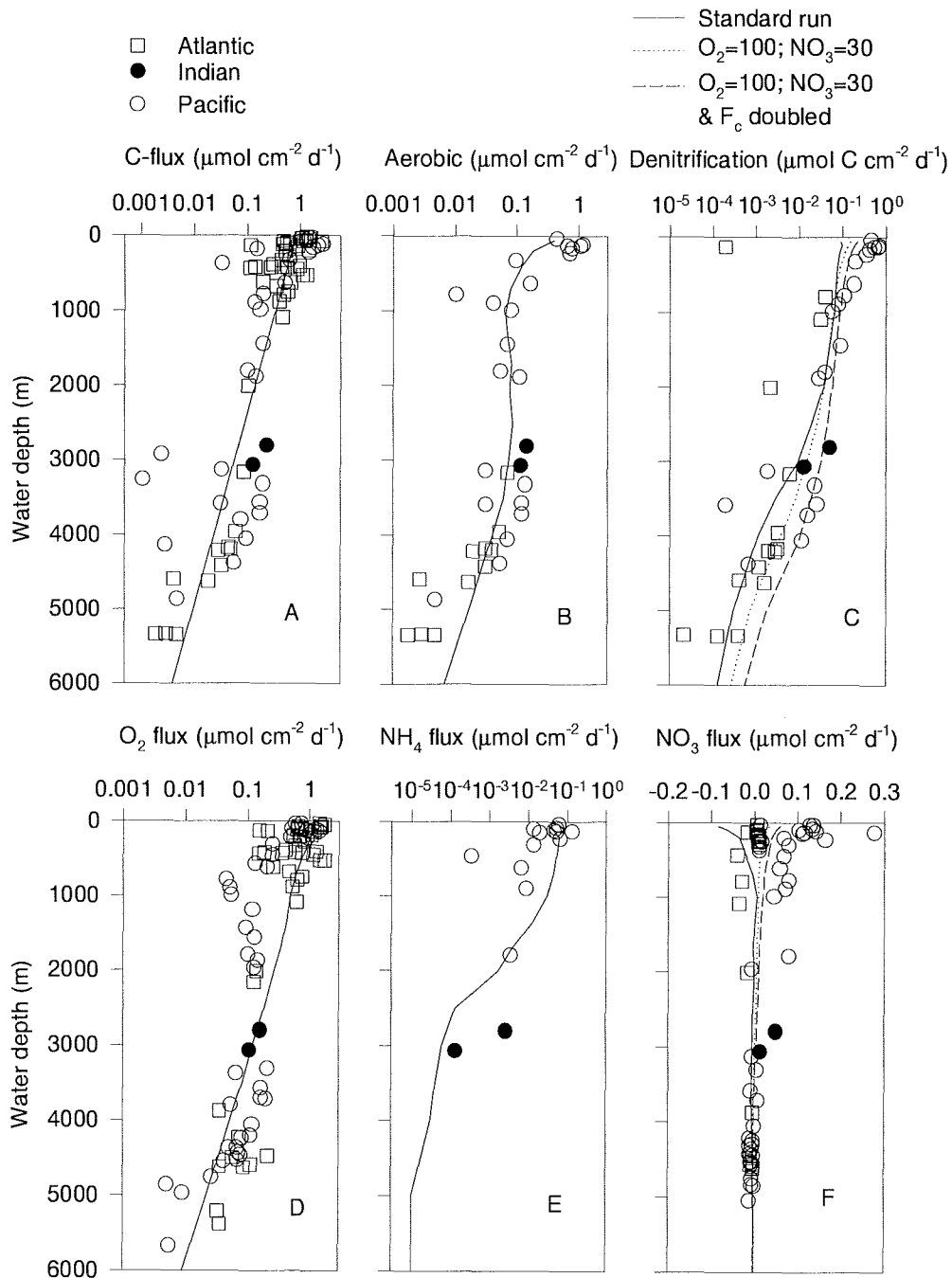
Figure 1. Comparison between estimated and literature-derived rates of benthic processes. Squares, solid circles and open circles indicate literature data from the Atlantic, Indian and Pacific Oceans, respectively. The solid lines show the model predicted rates and fluxes. (a) Rate of organic matter mineralization as a function of water depth. The solid line represents the exponential regression used to force the model. (b) Rate of aerobic mineralization as a function of water depth. (c) Denitrification rate as a function of water depth. The dotted and dashed lines indicate model results with $O_2 = 100$ μM and $NO_3 = 30$ μM, and with $O_2 = 100$ μM and $NO_3 = 30$ μM and doubled carbon fluxes, repectively. (d) Oxygen fluxes as a function of water depth. (e) Ammonium effluxes as a function of water depth. (f) Nitrate fluxes as a function of water depth. The dotted and dashed lines indicate model results with $O_2 = 100$ μM and $NO_3 = 30$ μM, and with $O_2 = 100$ μM and $NO_3 = 30$ μM and doubled carbon fluxes, repectively. Negative values are directed out of the sediment.

Table 2. Rates of Global Sedimentary Denitrification

Simulation Run	Total Ocean	Shelf
Standard	284.5	100.6
Diffusive bioturbation:		
$D_b/10$	285.8	97.4
$D_b/100$	232.1	62.8
$D_b \times 10$	247.1	89.6
$D_b \times 100$	217.9	64.1
Nonlocal exchange:		
f=0.46; x=4-4.9 cm	268.3	86.5
f=0.46; x=1.3-1.7 cm	280.3	96.5
f=0.46; x=5.9-7.2 cm	269.1	85.4
x=4-4.9 cm; f=1.58-0.16× ln(water depth)	225.7	60.8
NO_3-NH_4	318.0	109.9
$Kin_{O2}{}^{Denitr} = 1 \ \mu M$	246.7	90.3
Bottom water composition		
Arctic	272.2	120.1
Atlantic	240.2	85.1
Indian	297.4	98.8
Pacific	329.8	108.0
C/N ratio:		
Fast=6.6; slow=10	273.3	96.1
Fast=6.6; slow=20	256.0	89.3
Fast=8; slow =20	237.4	79.4
Carbon flux:		
$F_c/1.5$	206.8	75.1
$F_c/2$	161.0	58.6
$F_c/3$	108.2	37.9
$F_c \times 1.5$	385.5	128.8
$F_c \times 2$	477.4	148.2
$F_c \times 3$	636.2	186.8

See text for description of simulation runs. Units are in Tg N yr^{-1}.

organic carbon to the sediments (the dashed and dotted lines in Figures 1c and 1f).

Globally integrated rates of benthic processes can be obtained by combining bathymetric information from *Menard and Smith* [1966] with model rates as a function of depth. The global rate of sedimentary denitrification with the standard run totals about 285 Tg (T = 10^{12}) or 20.3 Tmol N yr^{-1}, with about 101 Tg yr^{-1} on the shelf (<150 m, Table 2).

3.2. Sensitivity Analysis

A Monte Carlo type sensitivity analysis by *Soetaert et al.* [1996a] including bottom water oxygen and nitrate concentrations, the sediment accumulation rate (ω), the diffusive bioturbation coefficient (D_b), the total flux of labile organic carbon (F_c), and the reactivity of organic carbon (k) revealed that bottom water oxygen and nitrate concentrations and the total flux of organic matter are the most important factors determining the relative contribution of denitrification in organic matter mineralization. In our sensitivity analysis we will address those parameters that might have changed during glacial/interglacial cycles (bottom water oxygen and nitrate concentrations and the flux and C/N ratio of organic matter) and those related to benthic organisms.

Increasing rates of diffusive bioturbation (D_b) at all depths with 1 or 2 orders of magnitude result in enhanced rates of anaerobic degradation at the expense of aerobic degradation. Conversely, decreasing D_b values at all depths cause enhanced rates of aerobic mineralization at the expense of anaerobic

pathways (Figure 2a and Table 2). Inclusion of nonlocal exchange of organic matter causes an enhancement of anaerobic degradation at the expense of aerobic degradation, with denitrification being depressed at all depth less than 3000 m (Figure 2a and Table 2). Rates of denitrification in deep-sea sediments are primarily carbon-limited and are consequently stimulated if moving organisms (either by enhancing D_b or nonlocal exchange) transport organic matter below the zone of oxygen penetration.

Moving organisms may also induce the formation of microenvironments with biogeochemical conditions different from those of the bulk sediments [*Aller*, 1982]. This sediment heterogeneity causes enhanced rates of nitrate turnover by shortening the distance between sites of aerobic nitrification and anaerobic denitrification. The degree of overlap in the model is determined by the denitrification oxygen-inhibition parameter ($Kin_{O2}{}^{Denitr}$), that is, the oxygen concentration at which denitrification proceeds at half the maximum speed. In the standard run, $Kin_{O2}{}^{Denitr}$ is 10 μM, and there is always some denitrification in the aerobic sediment layer (where nitrate is being produced) because of the hyperbolic functions used. Lowering $Kin_{O2}{}^{Denitr}$ to 1 μM separates the zones of nitrification and denitrification and results in lower rates of denitrification at all water depths (Figure 2b). Rates of denitrification in deep-sea sediments are particularly reduced because the diffusion distance from the separated zones of nitrification and denitrification is rather large, and denitrification will become even more carbon limited because it depends on what escapes aerobic mineralization.

Bender et al. [1989] proposed that nitrate may oxidize ammonium to nitrogen since this process is thermodynamically possible, and it is consistent with the often observed lack of ammonium in the zone of denitrification [*Emerson et al.*, 1980]. Moreover, *Soetaert et al.* [1996b] had to include this process in order to succesfully model the depth distribution of oxygen, nitrate, and ammonium in an eastern Pacific deep-sea site [*Reimers et al.*, 1992; *Cai et al.*, 1995]. Inclusion of this reaction using parameters obtained by *Soetaert et al.* [1996b] results in enhanced rates of denitrification at water depths less than 3000 m (Figure 2b). The global rate of sedimentary denitrification increases from 285 to 318 Tg N yr^{-1} (Table 2).

Estimated global rates of sedimentary denitrification with bottom water conditions similar to those found in the Arctic, Atlantic, Indian, and Pacific Oceans are 272, 240, 297, and 330 Tg N yr^{-1}, respectively (Table 2). These data indicate that small changes in the bottom water concentrations of nitrate and oxygen have a rather large impact on rates of benthic denitrification. To elaborate this sensitivity to bottom water conditions, sediments at water depths of 100, 1000, and 4000 m have been modeled as a function of bottom water oxygen and nitrate levels. The results for sediments at 1000-m water depth were qualitatively similar to those for sediments at 100 m and therefore not presented.

Increasing bottom water concentrations of oxygen enhances rates of nitrification and consequently decreases effluxes of ammonium (not shown). At low bottom water oxygen concentrations, nitrate is diffusing into the sediment (Figure 3), but at high oxygen levels, nitrate diffuses out of the sediment, irrespective of the bottom water nitrate concentration (in the range 10-30 μM). However, the magnitude of the nitrate influx and the oxygen concentration at which the sediment switches from influxes to effluxes of nitrate depend on the nitrate
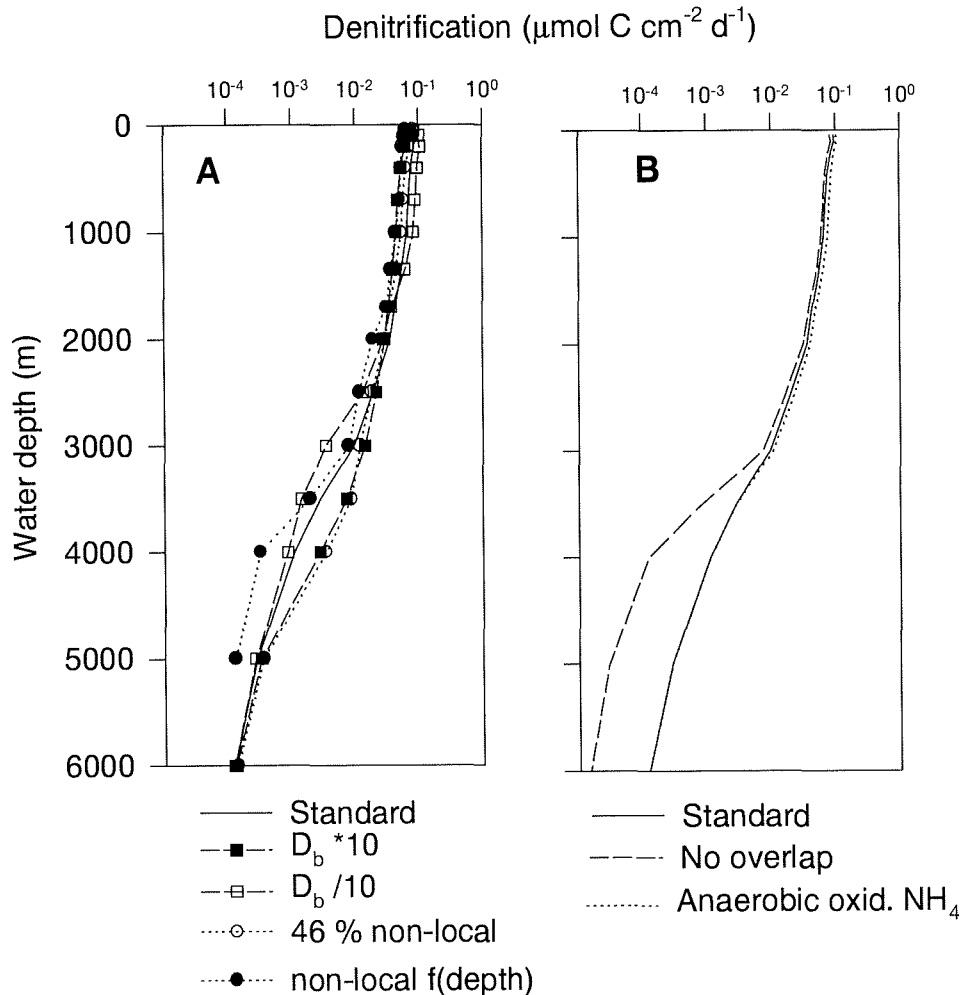
Denitrification (μmol C cm^{-2} d^{-1})

Legend (panel A):
— Standard
—■— D$_b$ *10
—□— D$_b$ /10
····○···· 46 % non-local
····●···· non-local f(depth)

Legend (panel B):
— Standard
——— No overlap
·········· Anaerobic oxid. NH$_4$

Figure 2. (a) Estimated rates of sedimentary denitrification as a function of water depth for standard run (solid line), runs with 10 times higher (solid squares and dashed line) or lower (open squares and dashed line) rates of diffusive bioturbation, and runs with nonlocal exchange processes included with 46% being injected between 4 and 4.9 cm (open circle and dotted line) and a fraction given by f=1.58-0.16 × ln(water depth) being injected between 4 and 4.9 cm (solid circle and dotted line). (b) Estimated rates of sedimentary denitrification as a function of water depth for standard run (solid line) and runs with no overlap between nitrification and denitrification ($Kin_{O2}{}^{Denitr}$ = 1 μM, dashed line) and with anaerobic oxidation of ammonium (nitrate reduction coupled to ammonium oxidation, dotted line).

concentration of the bottom water (Figure 3). Denitrification in deep-sea sediments decreases with increasing oxygen concentrations, because aerobic mineralization increases and removes most of the reactive carbon so that denitrification becomes carbon limited. In shelf sediments underlying nitrate-poor bottom water, denitrification increases with increasing oxygen concentrations because nitrification is stimulated and more nitrate becomes available. However, at high bottom water nitrate concentrations and increasing concentrations of oxygen there is a gradual shift from bottom water nitrate-supported denitrification to nitrification-coupled denitrification resulting in a rather constant level of sedimentary denitrification. These opposite effects of varying oxygen levels on sedimentary denitrification have been observed experimentally in laboratory freshwater sediments [Rysgaard et al., 1994].

Increasing bottom water concentrations of nitrate have very limited effects on rates of nitrification and on effluxes of ammonium (not shown). Increasing the bottom water nitrate concentrations causes a shift from nitrate effluxes at low nitrate levels to nitrate influxes at high nitrate levels for shelf sediments and for deep-sea sediments underlying oxygen-poor waters (Figure 4). Well-oxygenated deep-sea sediments remain nitrate exporting systems because aerobic processes dominate in these sediments. Denitrification rates increase with increasing concentrations of nitrate in the bottom water, mainly because of the trapping of nitrification-produced nitrate and partly because of nitrate influxes (Figure 4). Nitrification is a much more important nitrate source than bottom water nitrate, except for shelf sediments underlying oxygen-poor and nitrate-rich water.

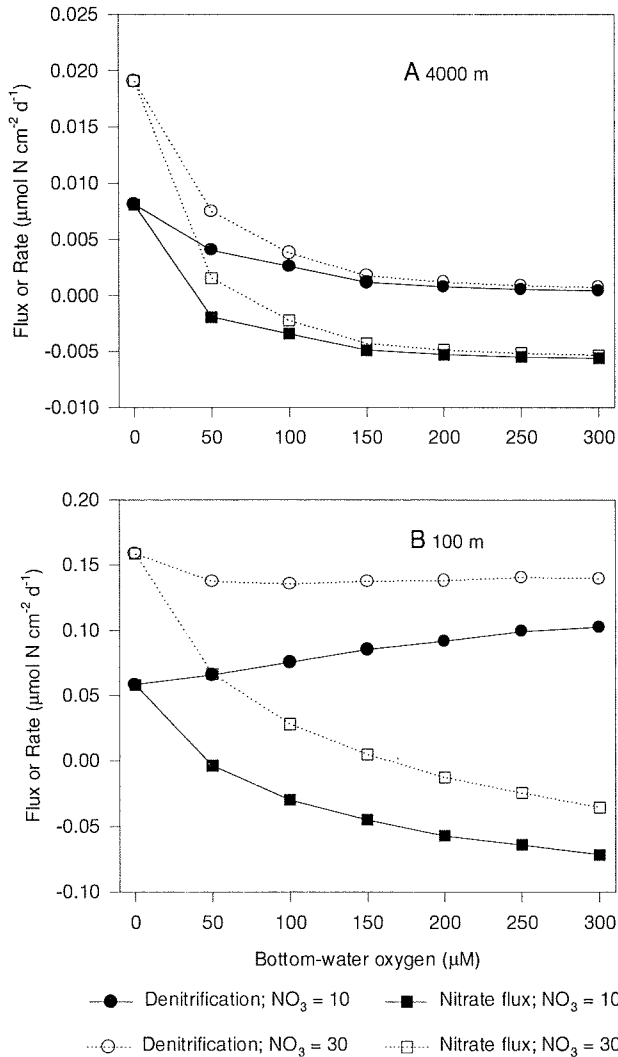Changes in the C/N ratio of decomposing organic matter have

Figure 3. Fluxes of nitrate (squares) and rates of denitrification (circles) in μmol N cm^{-2} d^{-1} as a function of bottom water oxygen concentrations for sediments at water depth of (a) 4000 and (b) 100 m. Solid lines indicate NO$_3$ = 10 μM; dotted lines indicate NO$_3$ = 30 μM. Negative fluxes indicate effluxes.

ratio of organic matter given the range of C/N ratios observed (7 to 12 [*Martin and Sayles*, 1994]).

Sedimentary denitrification is most sensitive to the rate of supply of labile organic carbon. Enhancing the carbon flux at all water depths with factors 1.5, 2, and 3 enhances the global sedimentary denitrification rates from 285 to 385, 477, and 636 Tg N yr^{-1}, respectively. Similarly, decreasing the carbon flux at all water depths with factors 1.5, 2, and 3 causes a decrease in sedimentary denitrification from 285 to 207, 161, and 108 Tg N yr^{-1}, respectively (Table 2). This almost proportional response of denitrification rates to carbon supply rates becomes evident if the global rates of sedimentary carbon mineralization and denitrification are compared (Figure 5). Denitrification accounts for 11% to 7% of the global sedimentary carbon mineralization at low (1000 Tg C yr^{-1}) and high (9700 Tg C yr^{-1}) loadings, respectively.
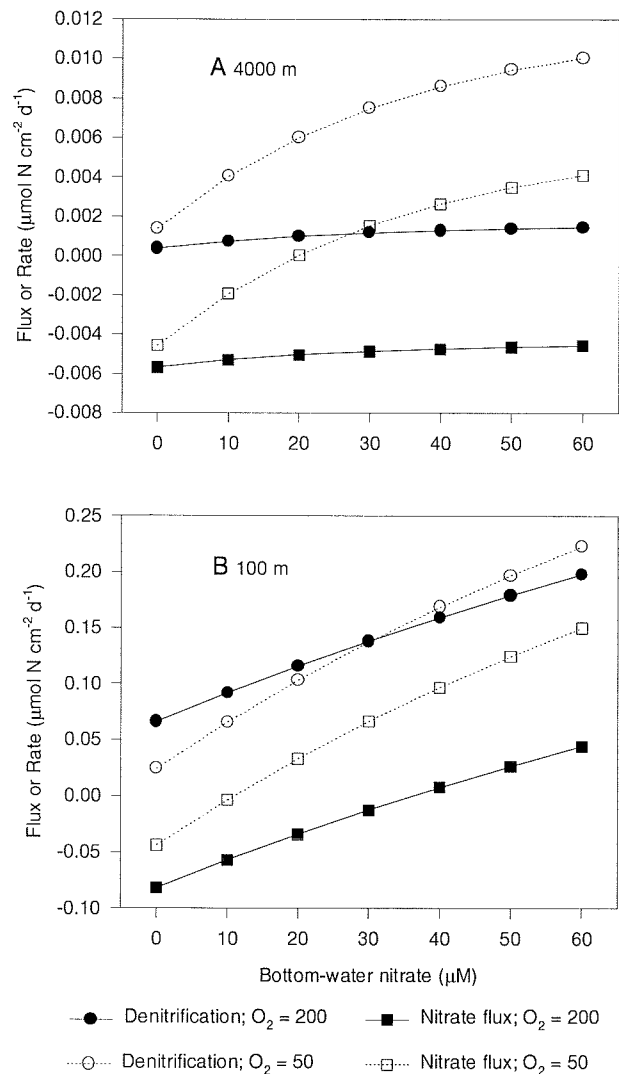

Figure 4. Fluxes of nitrate (squares) and rates of denitrification (circles) in μmol N cm^{-2} d^{-1} as a function of bottom water nitrate concentrations for sediments at water depth of (a) 4000 and (b) 100 m. Solid lines indicate O$_2$ = 200 μM; dotted lines indicate O$_2$ = 50 μM. Negative fluxes indicate effluxes.

a rather limited effect on rates of sedimentary denitrification. In the standard run the molar C/N ratios of the fast and slowly decomposing organic fractions are 6.6 and 7.5, respectively, with the consequence that the C/N ratio of labile organic matter arriving at the sediment surface varies from 6.85 at 100 m to 7.0 at 4000 m water depth. Increasing the C/N ratio of the slowly decomposing fraction from 7.5 to 20 enhances the C/N ratio of the organic matter being decomposed (8.1 at 100 m water depth and 9.6 at 4000 m water depth) and lowers the global rate of denitrification from 285 to 256 Tg N yr^{-1} (Table 2). Also increasing the C/N ratio of the fast decaying fraction from 6.6 to 8 results in a global sedimentary denitrification rate of 237 Tg N yr^{-1} (Table 2). The labile organic matter arriving at the sediment-water interface then has C/N ratios that vary from 9.6 at 100 m to > 11 at 4000 m water depth. Accordingly, rates of sedimentary denitrification do not depend strongly on the C/N
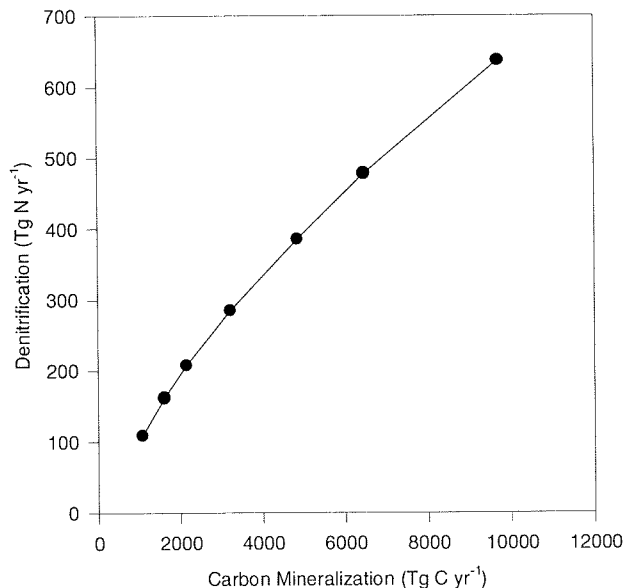
Figure 5. Relationship between globally integrated rates of benthic mineralization and benthic denitrification for seven model scenarios.

3.3. Sediments: A Source or Sink of N?

Particulate nitrogen arriving at the sediment may either become buried or be mineralized and returned to the water column as nitrate, ammonium, or nitrogen. Sediments may constitute a source of nitrogen (nitrate and ammonium) with respect to the water column but a sink of nitrogen because of denitrification and burial. Sediments may also act as a sink of nitrate if nitrate influxes occur. Figure 6 shows the model-generated benthic nitrogen fluxes in shelf (100 m), slope (1000 m), and deep-sea (4000 m) environments and that of shelf and slope sediments underlying nitrate-rich (40 μM) and oxygen-poor (80 μM) bottom waters. Sediments generally act as a source of nitrate to the bottom water, except for slope sediments (1000-2000 m, Figures 1f and 6c) and sediments underlying high-nitrate-low-oxygen (HNLO) waters (Figures 6b and 6d). These HNLO environments are mainly restricted to upwelling settings and along eastern boundaries of the ocean. Recent studies of California Borderland Basins [*Berelson et al.*, 1987; *Bender et al.*, 1989; *Jahnke*, 1990] and the Washington shelf and slope [*Devol*, 1991; *Devol and Christensen*, 1993] have shown that these sediments are, indeed, net sinks for nitrogen.

As a consequence of nitrate effluxes, denitrification is primarily coupled to nitrification. In slope sediments and sediments underlying HNLO waters there is denitrification depending on net diffusion of nitrate into the sediments, but even in these two settings, nitrification remains an important source of substrate for denitrifiers. Nitrification supplies more than 90% of the nitrate in slope sediments and more than 60% in HNLO environments (Figures 3, 4, and 6). This limited net contribution of bottom water nitrate to sedimentary denitrification does not indicate that bottom water nitrate concentrations have a small effect on benthic denitrification. At high bottom water concentrations of nitrate the net flux of nitrate out of the sediments is reduced in proportion to the reduction of

the concentration gradient; hence more nitrate becomes available for denitrification (Figure 4).

3.4. Extraction of a Metamodel

Rates of benthic denitrification are most sensitive to the sedimentation of labile organic carbon and bottom water concentrations of oxygen and nitrate (Table 2 and Figures 3, 4, and 5). The high sensitivity toward these three parameters makes it possible to derive a metamodel, that is, a regression-based model that can reproduce the results of the full diagenetic model to some extent. Such a metamodel can easily be incorporated into global biogeochemical cycling models and can be used to predict denitrification rates in the absence of detailed information.

Two thousands sets of parameter values were randomly chosen within a specified interval using a uniform (bottom water oxygen and nitrate concentrations) or log-uniform (water depth and labile carbon flux) Latin hypercube sampling procedure and were used in model runs with the standard model to obtain a training set for the metamodel. Bottom water oxygen and nitrate concentrations were varied between 10 and 350 μM and 1 and 60 μM, respectively. The carbon flux was allowed to vary within 2 orders of magnitude at each water depth (i.e., the minimum value equals mean rate/10 and maximum equals mean rate $\times$ 10) and water depth was in the range 50-6000 m. This log-transformed resampling procedure for carbon fluxes and water depths was used to better cover the overall range, in particular, the shallow and high carbon flux environments where rates of denitrification rates are highest.

Multiple regression analysis of these model runs indicates that denitrification can be predicted with (r^2 = 0.921 and s^2 = 0.062)

$$\log (Den) = -0.9543 + 0.7662 \times \log(F_c) - 0.2350 \times \log(F_c) \times \log(F_c),$$

or even better with (r^2 = 0.976 and s^2 = 0.019)

$$\log (Den) = -2.2567 - 0.1850 \times \log(F_c) - 0.2210 \times \log(F_c) \times \log(F_c) - 0.3995 \times \log(NO_3) \times \log(O_2) + 1.2500 \times \log(NO_3) + 0.4721 \times \log(O_2) - 0.0996 \times \log (Z) + 0.4256 \times \log(F_c) \times \log(O_2)$$

where (O_2) and (NO_3) are the bottom water concentrations in micromolars, (F_c) (labile carbon flux) and (Den) (denitrification rate) are in μmol C cm^{-2} d^{-1}, and (Z) is water depth in meters. A lognormal regression was used to assure physically real, that is, positive denitrification rates. The metamodel and full diagenetic model are compared in Figure 7. The significant dependence on bottom water oxygen and nitrate and the flux of organic carbon and their interactions are consistent with the results shown in Figures 3, 4, and 5. Inclusion of a quadratic dependence on carbon fluxes significantly improved the predictability. This quadratic term accounts for the nonlinear contribution of denitrification to carbon mineralization (Figure 8). At low carbon fluxes, aerobic mineralization dominates and denitrification may account for about 1% to 10% of the mineralization. At intermediate carbon fluxes, rates of denitrification and anaerobic mineralization increase at the expense of aerobic mineralization. At high carbon fluxes, anaerobic mineralization increases at the expense of aerobic mineralization and denitrification.
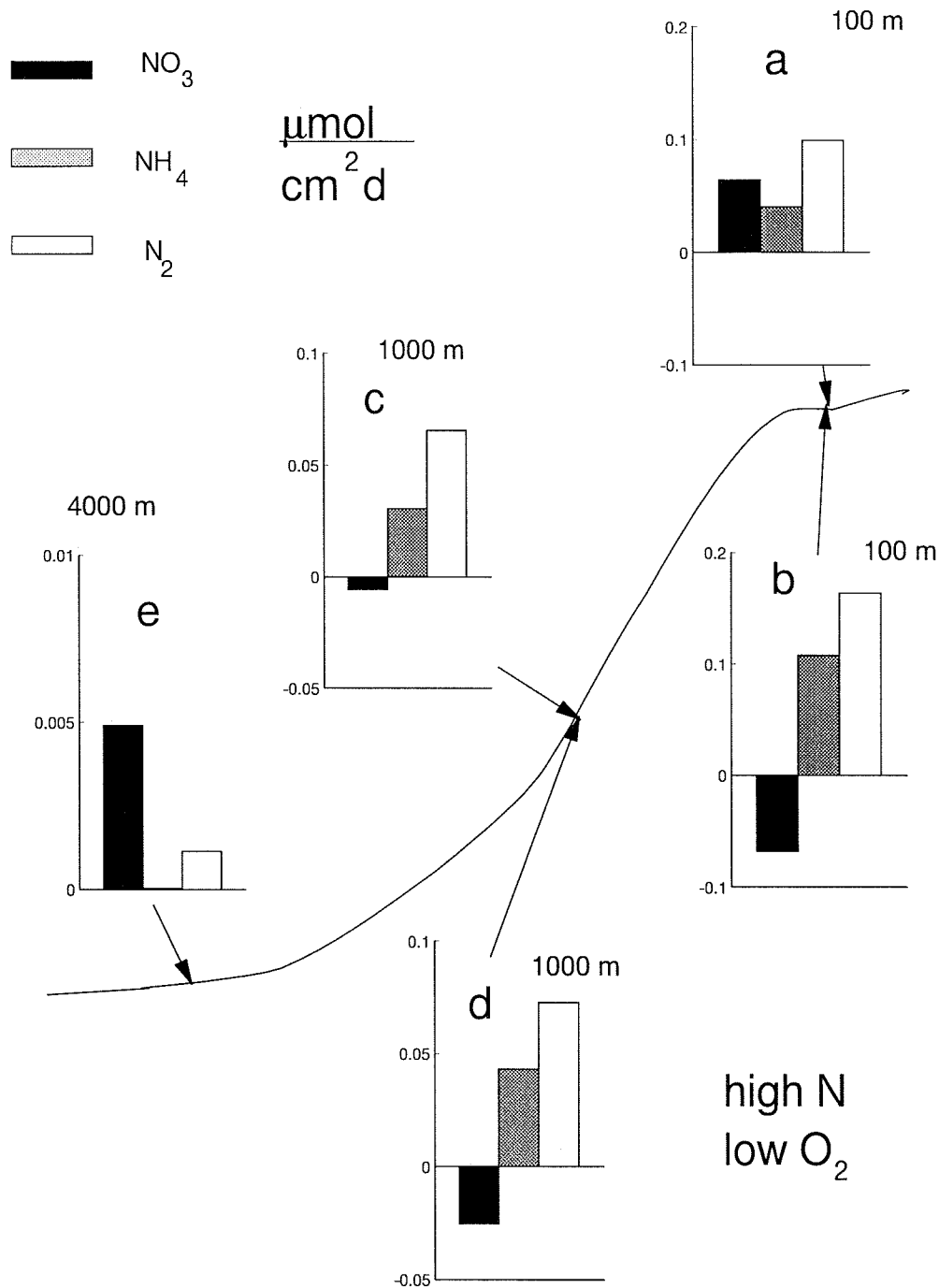
Figure 6. Benthic nitrogen fluxes along the ocean margin for "normal" bottom waters (upper left) and high-nutrient-low-oxygen (HNLO) bottom waters (lower right) (a) 100 m, (b) 100 m with HNLO bottom waters, (c) 1000 m, (d) 1000 m with HNLO bottom waters, and (e) 4000 m. Nitrogen fluxes are in μmol N cm^{-2} d^{-1}.

4. Discussion

4.1. Global Rate of Sedimentary Denitrification

The global rate of sedimentary denitrification estimated in this study (285 Tg N yr^{-1}) is significantly higher than values reported hitherto in the literature which range from 12 to 89 Tg N yr^{-1} (Table 3). It is therefore instructive to discuss the validity of our estimate and to discuss why it is so much higher than other estimates. There are three lines of support for our high estimate of global sedimentary denitrification.

First, predicted rates of denitrification of our standard run are close to the data reported in the literature, though the variability
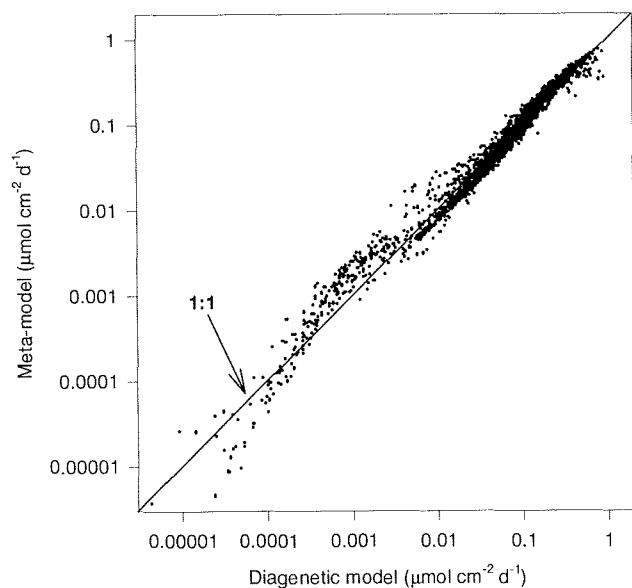
Figure 7. Comparison of denitrification rates (μmol C cm^{-2} d^{-1}) between full diagenetic model and metamodel.

Table 3. Comparison of Global Rates of Sedimentary Denitrification

Source	Total Ocean	Shelf
Liu and Kaplan [1984]	11.9	4.9
Hattori [1983]	44	41[a]
Jørgensen [1983]	82	55
Codispoti and Christensen [1985] and Christensen [1994]	69	62[a]
Chistensen et al. [1987]	89	81[a]
This study	285	101

Units are in Tg N yr^{-1}.
[a] Including estuaries (about 12 Tg N yr^{-1}).

in the data allows considerable variability in model estimates (Figure 1c). Moreover, model-predicted denitrification rates are rather conservative estimates of the true rates, since modeled rates generally are lower than reported rates (Figure 1c) and because most of the denitrification rates reported in the literature need a significant upward revision [Devol, 1991].

Second, our estimated global rate of denitrification in shallow sediments (< 150 m) is about 100 Tg N yr^{-1}, which is in line

with more recent estimates for continental shelf sediments (69 Tg N yr^{-1} [Christensen et al., 1987] and 100 Tg N yr^{-1} [A. Devol, personal communication, 1996]). Moreover, our estimates of denitrification in shelf sediments (0.087-0.100 μmol N cm^{-2} d^{-1}) are in the center of the range of recently reported rates of benthic denitrification in the North Sea based on the nitrogen isotope pairing technique (0.024-0.032 μmol N cm^{-2} d^{-1} [Lohse et al., 1996]), the Gulf of Maine based on water column nutrient budgets (0.069-0.104 μmol N cm^{-2} d^{-1} [Christensen et al., 1996]), and the Washington shelf based on in situ nitrogen flux measurements (0.078-0.53 μmol N cm^{-2} d^{-1} [Devol, 1991]).

Third, according to our model calculations, denitrification accounts for about 7-11% of the global organic matter mineralization (Figure 5). The estimated contribution of denitrification to organic matter decomposition (Figure 8) varies from about 1% to 10% at low carbon loadings (< 0.01 μmol cm^{-2} d^{-1}) to about 7% to 30% at intermediate carbon loadings (0.1 to 1 μmol cm^{-2} d^{-1}). This range is consistent with reported diagenetic model estimates (3.7% to 9.4% [Boudreau, 1996]), electron flow budgets (3% to 20% [Jørgensen, 1983]), and summaries of diagenetic pathways (deep-sea sediments, 1% to 7% and slope and rise sediments, 8% to 25% [Middelburg et al., 1993] and coastal systems and estuaries, 3% to 37 % [Heip et al., 1995]).

Our model estimates are therefore consistent with recent data for the continental shelf but deviate from previous reports on denitrification in slope and deep-sea sediments. Reported estimates for slope and deep-sea sediments originate from Liu and Kaplan [1984] and Hattori [1983]. Liu and Kaplan [1984] have estimated global benthic denitrification in slope and deep-sea sediments (7 Tg N yr^{-1}) by combining the areal distribution of organic carbon concentrations [Premuzic et al., 1982] with a regression of the first-order rate constant of denitrification on organic carbon concentrations. Their estimate is biased toward deep-sea sediments, and moreover, denitrification was estimated from the net flux of nitrate into the deeper layers of the sediment thus excluding nitrification as a major nitrate source. The estimate of Hattori [1983] (3 Tg N yr^{-1}) is based on very few data and on the assumption that only one third of the open ocean area has sediments where denitrification is taking place. It is clear that these previous approaches result in a severe underestimation of denitrification rates in slope and deep-sea sediments.

The sensitivity analysis has shown that denitrification is most sensitive to the total rate of mineralization and bottom water conditions (Table 2). Integrated rates of sedimentary denitrifica-
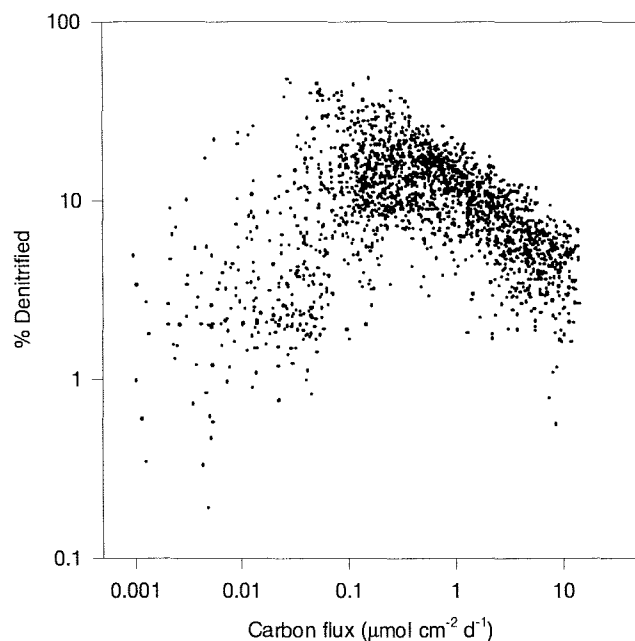

Figure 8. The relative contribution of denitrification to organic matter mineralization as a function of the total mineralization rate (μmol C cm^{-2} d^{-1}) as obtained during the Monte Carlo simulation.

tion for the individual ocean basins based on their average bottom water conditions and surface areas are 44.1, 73.9, 45.0, and 133.8 Tg N yr^{-1} for the Arctic, Atlantic, Indian, and Pacific Oceans, respectively. Summation of integrated denitrification rates for individual basins yields a global rate of 296.8 Tg N yr^{-1}, an estimate rather similar to that based on globally averaged bottom water conditions (285 Tg N yr^{-1}).

Any error in our estimate of the total mineralization rate will propagate into our estimate for the global rate of sedimentary denitrification. Estimates of global benthic mineralization range from about 2300 Tg C yr^{-1} [Jørgensen, 1983] to 2600 Tg C yr^{-1} [Smith and Hollibaugh, 1993]. The first estimate is based on oxygen consumption rates and may be 10% to 25% too low because of storage of reduced components, mainly iron sulfides, and escape of nitrogen [Heip et al., 1995]. By combining these independent estimates of global mineralization with the relation between denitrification and mineralization shown in Figure 5, we obtain global dentrification rates of about 210 and 232 Tg N yr^{-1}, respectively. If the estimate of Jørgensen [1983] is corrected with 10% to 25% for incomplete re-oxidation of reduced components, we obtain global sedimentary denitrification rates of 227 and 251 Tg N yr^{-1}, respectively. Accordingly, the most likely estimate for global benthic denitrification is between 230 and 285 Tg N yr^{-1}.

4.2. Implications

The significant upward revision of benthic denitrification rates from 12-89 Tg N yr^{-1} to 230-285 Tg N yr^{-1} demands a reconsideration of the marine nitrogen budget (Table 4). The sum of reported nitrogen sources (90-293 Tg N yr^{-1}) is much smaller than the total of nitrogen sinks (318-418 Tg N yr^{-1}) indicating a large imbalance in the marine nitrogen budget. Our estimate for nitrogen sources already includes the provocative upwardly revised biological nitrogen fixation rate (40-120 Tg N
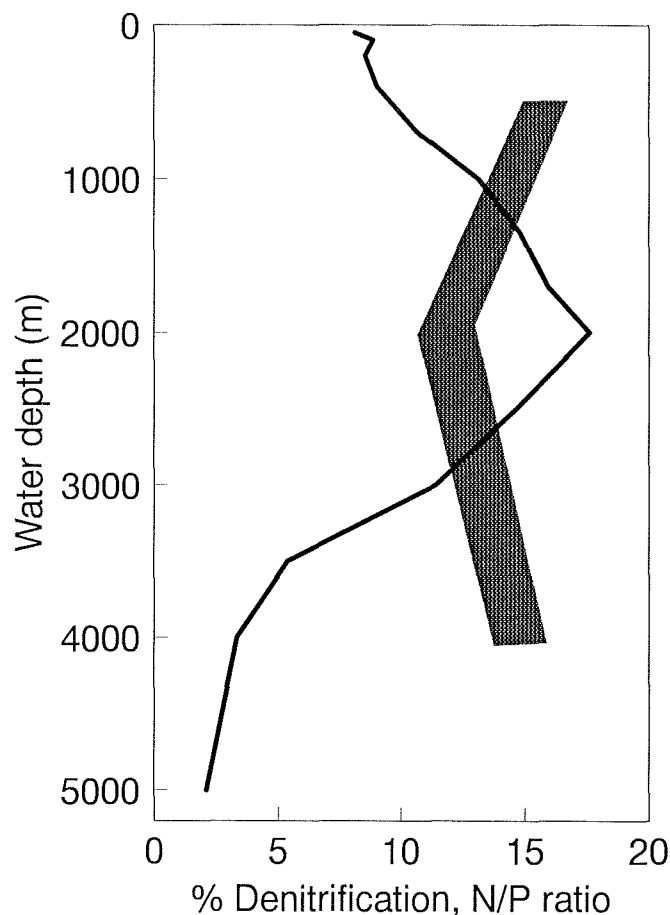

Figure 9. The relative contribution of denitrification in organic matter mineralization and the range of N/P remineralization ratios reported by *Anderson and Sarmiento* [1994] as a function of water depth.

Table 4. Marine Fixed Nitrogen Budget

Process	Rate	References
Inputs		
Riverine	25-43	1, 2, 3, 4
Atmospheric, including rain	40-50	2, 4, 5, 6
Nitrogen fixation, classical	25-30	4, 5, 6
Nitrogen fixation, tentative	40-200	3, 7
Totals	90-293	
Outputs		
Burial	10-27	2, 4, 5, 8
Organic nitrogen and ammonia export	13-16	3, 4, 5
Denitrification		
Water column	60-90	3, 5, 6, 9
Sediments	230-285	this study
Totals	313-418	
Fixed nitrogen inventory, Tg N	720300	10
Residence time inputs, 10^3 years	2.5-8	
Residence time outputs, 10^3 years	1.7-2.3	

Rates are in Tg N yr^{-1}. 1, *Meybeck* [1982]; 2, *Schlesinger* [1991]; 3, *Galloway et al.* [1995]; 4, *Codispoti and Christensen* [1985]; 5, *Christensen* [1994]; 6, *Devol* [1991]; 7, *Carpenter and Romans* [1991]; 8, *Wollast* [1991]; 9, *Ganeshram et al.* [1995]; and 10, *Mackenzie et al.* [1993].

yr^{-1}) of *Carpenter and Romans* [1991]. These enhanced nitrogen input and output terms relate to residence times varying from 2.5 to 8 × 10^3 years and from 1.7 to 2.3 × 10^3 years, respectively (Table 4). These reduced residence timescales imply that the oceanic nitrogen cycle might change over shorter timescales than previously assumed.

The upward revision of sedimentary denitrification rates also has implications for oceanic N/P remineralization ratios. Below 1000 m and at all depths along continental margins, benthic mineralization contributes significantly to oceanic mineralization [Jahnke et al., 1990]. Aerobic mineralization in sediments, like water column mineralization, results in N/P remineralization ratios similar to the N/P ratio of the incoming labile organic matter. However, sedimentary denitrification results in a loss of nitrogen relative to phosphorus. The modeled relative contribution of denitrification to sedimentary mineralization initially increases from about 8% in shelf sediments to a maximum of 18% at 2000 m but then decreases to less than 5% at depths more than 3500 m (Figure 9). On the basis of a nonlinear inversion analysis of nutrient data, *Anderson and Sarmiento* [1994] reported that N/P ratios of remineralization decrease with depth from a value of 16 at 400 m to a value of 12 at 2000 m and then increase again to about 15 at 4000 m, as

Table 5. Summary of Glacial Conditions and Expected Effects on Sedimentary Denitrification

Change	Expected Effect
Sea level drop; reduction in shelf area	Reduction of denitrification in shelf sediments
Reduced water column denitrification	Increased water column nitrate inventory; enhanced benthic denitrification
More sluggish circulation	Lower oxygen concentrations in deep-sea water; enhanced denitrification in deep-sea sediments
Higher new production	Enhanced carbon fluxes; enhanced rates of sedimentary denitrification

shown schematically in Figure 9. The N/P remineralization ratio almost perfectly mirrors the relative contribution of denitrification (Figure 9) and this trend in the N/P remineralization ratio may therefore, indeed, be related to sedimentary denitrification, as suggested by *Anderson and Sarmiento* [1994]. However, the decrease in N/P ratios from 16 to 12 can only be accounted for if (1) denitrification accounts for at least 25% of the sedimentary mineralization and if (2) all mineralization occurs in sediments rather than in the water column at these depths. Although the former condition is not met in our standard model predictions, the difference is small and it is well within the variability of available data (see also Figure 8). If sedimentary denitrification accounts for a major part of the oceanic carbon utilization at intermediate depths, it should also have some impact on O_2/P regeneration ratios since less oxygen is consumed per unit of organic matter mineralized. The data presented by *Anderson and Sarmiento* [1994, Figure 2] do, indeed, show a minimum in the O_2/P regeneration ratio at 2000 m depth in the Atlantic and Indian Oceans but not in the Pacific Ocean.

Rates of benthic denitrification are most sensitive to carbon fluxes and bottom water concentrations of oxygen and nitrate (Table 2 and Figures 3, 4, and 5). These parameters are also the ones that are likely to exhibit considerable changes on glacial-interglacial timescales (Table 5).

During the last glacial the sea level dropped more than 100 m, and the area of continental shelf sediments was significantly reduced with a concomitant decrease in rates of sedimentary denitrification [*Berger and Keir*, 1984]. This mechanism could potentially lower the nitrogen output with 100 Tg N yr^{-1}. *Shäfer and Ittekkot* [1993], *Altabet et al.* [1995], and *Ganeshram et al.* [1995] have used the downcore distributions in $^{15}N/^{14}N$ ratios of organic matter to argue that water column denitrification was lower during glacial periods. This reduction of denitrification in shelf sediments and in the water column in the Pacific and Indian Oceans, may have increased the oceanic nitrate inventory, assuming all other sources and sinks are invariant. Such an increase in nitrate concentrations may have stimulated the biological pump with consequent enhanced carbon fluxes to the sediment and may have lowered atmospheric carbon dioxide concentrations.

However, this assumption of invariance may perhaps not be valid for sedimentary denitrification in slope and deep-sea sediments, because higher bottom water concentrations of nitrate cause enhanced rates of denitrification (Figure 4). Moreover, glacial ocean ventilation may have been more sluggish than today, with the result that bottom water oxygen concentrations were lower in the deep sea [*Toggweiler and Sarmiento*, 1984].

Lower oxygen levels are expected to enhance the rate of denitrification in deep-sea sediments (Figure 3a). Furthermore, there are several indications for enhanced rates of new production and higher carbon fluxes to the sediments during glacial times [e.g., *Sarnthein et al.*, 1988; *Kumar et al.*, 1995]. Enhanced glacial carbon fluxes would also have enhanced rates of sedimentary denitrification (Figure 5). Accordingly, it might well be possible that during the last glacial, reduced rates of denitrification in shelf sediments and the water column were balanced by enhanced rates of denitrification in slope and deep-sea sediments. This interglacial-glacial shift in sites of denitrification provides a buffering mechanism for nitrogen in the ocean and requires further study with coupled biogeochemical models including the ocean and its sediments.

References

Aller, R.C., The effects of macrobenthos on chemical properties of marine sediment and overlying water, in *The Biotic Alteration of Sediments*, edited by P.L. McCall and M.J. Tevesz, pp. 53-102, Plenum, New York, 1982.

Altabet, M.A., R. Francois, D.W. Murray, and W.L Prell, Climate-related variations in denitrification in the Arabian Sea from sediment $^{15}N/^{14}N$ ratios, *Nature, 373*, 506-509, 1995.

Anderson, L.A., and J.L. Sarmiento, Redfield ratios of remineralization determined by nutrient data analysis, *Global Biogeochem. Cycles, 8(1)*, 65-80, 1994.

Archer, D., and A. Devol, Benthic oxygen fluxes on the Washington shelf and slope: A comparison of in situ microelectrode and chamber flux measurements, *Limnol. Oceanogr., 37*, 614-629, 1992.

Barnola, J.M., D. Raynaud, Y.S. Korotkevich, and C. Lorius, Vostok ice core provides 160,000-year record of atmospheric CO_2, *Nature, 329*, 408-411, 1987.

Bender, M.L., R. Jahnke, R. Weiss, W. Martin, D.T. Heggie, J. Orchardo, and T. Sowers, Organic carbon oxidation and benthic nitrogen and silica dynamics in San Clemente Basin, a continental borderland site, *Geochim. Cosmochim. Acta, 53*, 685-697, 1989.

Berelson, W.M., D.E. Hammond, and K. S. Johnson, Benthic fluxes and the cycling of biogenic silica and carbon in two southern California borderland basins, *Geochim. Cosmochim. Acta, 51*, 1345-1363, 1987.

Berger, W.H., and R.S. Keir, Glacial-Holocene changes in atmospheric CO_2 and the deep-sea record, in *Climate Processes and Climate Sensitivity, Geophys. Monogr. Ser*, vol. 29, edited by J.E. Hansen and T. Takahashi, pp. 337-351, AGU, Washington, D. C., 1984.

Berner, R.A., *Early Diagenesis - A Theoretical Approach*, Princeton Univ. Press, Princeton, N. J., 1980.

Boudreau, B.P., On the equivalence of nonlocal and radial-diffusion models for porewater irrigation, *J. Mar. Res., 47*, 731-735, 1984.

Boudreau, B.P., A method-of-lines code for carbon and nutrient diagenesis in aquatic sediments, *Comput. Geosc., 22*, 479-496, 1996.

Broecker, W.S., Glacial to interglacial changes in ocean chemistry, *Prog. Oceanogr., 11*, 151-197, 1982.

Cai, W.-J., C.E. Reimers, and T. Shaw, Microelectrode studies of organic carbon degradation and calcite dissolution at a California continental rise site, *Geochim. Cosmochim. Acta, 59*, 497-511, 1995.

Carpenter, E.J., and K. Romans, Major role of the cyanobacterium *Trichodesmium* in nutrient cycling in the North Atlantic Ocean, *Science, 254*, 1356-1358, 1991.

Christensen, J.P., Carbon export from continental shelves, denitrification and atmosphere carbon dioxide, *Cont. Shelf Res., 14(5)*, 547-576, 1994.

Christensen, J.P., J. W. Murray, A.H. Devol, and L.A. Codispoti, Denitrification in continental shelf sediments has major impact on the oceanic nitrogen budget, *Global Biogeochem. Cycles, 1(2)*, 97-116, 1987.

Christensen, J.P., D.W. Townsend, and J.P. Montoya, Water column nutrients and sedimentary denitrification in the Gulf of Maine, *Cont. Shelf Res., 16(4)*, 489-515, 1996.

Codispoti, L.A., Is the ocean losing nitrate?, *Nature, 376*, 724, 1995.

Codispoti, L.A., and J.P. Christensen, Nitrification, denitrification and nitrous oxide cycling in the eastern tropical South Pacific Ocean, *Mar. Chem., 16*, 277-300, 1985.

Devol, A., Direct measurement of nitrogen gas fluxes from continental shelf sediments, *Nature, 349*, 319-321, 1991.

Devol, A.H., and J. P. Christensen, Benthic fluxes and nitrogen cycling in sediments of the continental margin of the eastern North Pacific, *J. Mar. Res., 51*, 345-372, 1993.

Emerson, S., R. Jahnke, M. Bender, P. Froelich, G. Klinkhammer, C. Bowser, and G. Setlock, Early diagenesis in sediments from the eastern equatorial pacific, 1, pore water nutrient and carbonate results, *Earth Planet. Sci. Lett., 49*, 57-80, 1980.

Fanning, K.A., Nutrient provinces in the sea: Concentration ratios, reaction rate ratios, and ideal covariation, *J. Geophys. Res., 94(4)*, 5693-5712, 1992.

Galloway, J.N., W.H. Schlesinger, H. Levy II, A. Michaels, and J.L. Schnoor, Nitrogen fixation: Anthropogenic enhancement-environmental response, *Global. Biogeochem. Cycles, 9(2)*, 235-252, 1995.

Ganeshram, R.S., T.F. Pedersen, S.E. Calvert, and J.W. Murray, Large changes in oceanic nutrient inventories from glacial to interglacial periods, *Nature, 376*, 755-758, 1995.

Hattori, A., Denitrification and dissimilatory nitrate reduction. in *Nitrogen in the Marine Environment*, edited by E. Carpenter and D.B. Capone, pp. 191-232, Academic , San Diego, Calif., 1983.

Heip, C.H.R., N.K. Goosen, P.M.J. Herman, J. Kromkamp, J.J. Middelburg, and K. Soetaert, Production and consumption of biological particles in temperate tidal estuaries. *Oceanogr. Mar. Biol., 33*, 1-150, 1995.

Jahnke, R. A., Early diagenesis and recycling of biogenic debris at the seafloor, Santa Monica Basin, California, *J. Mar. Res., 48*, 413-436, 1990.

Jahnke, R.A., C.E. Reimers, and D.B. Craven, Intensification of recycling of organic matter at the seafloor near ocean margins, *Nature, 348*, 50-54, 1990.

Jørgensen, B. B., Processes at the sediment-water interface, in *The Major Biogeochemical Cycles and Their Interactions*, edited by B. Bolin and R. B. Cook, pp. 477-509, Wiley, New York, 1983.

Kumar, N., R.F. Anderson, R.A. Mortlock, P.N. Froelich, P. Kubik, B. Dittrich-Hannen, and M. Suter, Increased biological productivity and export production in the glacial Southern Ocean, *Nature, 378*, 675-680, 1995.

Liu, K.-K., and I.R. Kaplan, Denitrification rates and availability of organic matter in marine environments, *Earth Planet. Sci. Lett., 68*, 88-100, 1984.

Lohse, L., H.T. Kloosterhuis, W. van Raaphorst, and W. Helder, Denitrification rates as measured by the isotope pairing method and by the acetylene inhibition technique in continental shelf sediments of the North Sea, *Mar. Ecol. Prog. Ser., 132*, 169-179, 1996.

Mackenzie, F.T., L.M. Ver, C. Sabine, M. Lane, and A. Lerman, C, N, P, S global biogeochemical cycles and modelling of global change, in *Interactions of C, N, P and S Biogeochemical Cycles and Global Change*, edited by R. Wollast, F. T. Mackenzie, and L. Chou, pp. 1-61, Springer-Verlag, New York, 1993.

Martin, W.R., and F.T. Sayles, Seafloor diagenetic fluxes, in *Material Fluxes on the Surface of the Earth*. pp. 143-163, Nat. Acad. Press, Washington, D. C., 1994.

McElroy, M.B., Marine biological controls on atmospheric CO_2 and climate, *Nature, 302*, 328-329, 1983.

Menard, H.W., and S.M. Smith, Hypsometry of ocean basin provinces, *J. Geophys. Res., 71(18)*, 4305-4325, 1966.

Meybeck, M., Carbon, nitrogen and phosphorus transport by world rivers, *Am. J. Sci., 282*, 401-450, 1982.

Middelburg, J.J., T. Vlug, and F.J.W.A. van der Nat, Organic matter mineralization in marine systems, *Global Planet. Change, 8*, 47-58, 1993.

Middelburg, J.J., K. Soetaert, and P.M.J. Herman, Empirical relationships for use in global diagentic models, *Deep Sea Res.*, in press, 1996.

Premuzic, E.T., C.M. Benkovitz, J.S. Gaffney, and J.J. Walsh, The nature and distribution of organic matter in the surface sediments of the world oceans and seas, *Org. Geochem., 4*, 63-77, 1982.

Reimers, C.E., R.A. Jahnke, and D.C. McCorkle, Carbon fluxes and burial rates over the continental slope and rise off central California with implications for the global carbon cycle, *Global Biogeochem. Cycles., 6(2)*, 199-224, 1992.

Rysgaard, S., N. Risgaard-Petersen, N. P. Sloth, K. Jensen, and L.P. Nielsen, Oxygen regulation of nitrification and denitrification in sediments, *Limnol. Oceanogr., 39*, 1643-1652, 1994.

Sarnthein, M., K. Winn, J.-C. Duplessy, and M.R. Fontugne, Global variations of surface ocean productivity in low and mid latitudes: Influence on CO_2 reservoirs of the deep ocean and atmosphere during the last 21,000 years, *Paleoceanography, 3(3)*, 361-399, 1988.

Schlesinger, W.H., *Biogeochemistry*, Academic, San Diego, Calif., 1991.

Shäfer, P., and V. Ittekkot, Seasonal variability of $\delta^{15}N$ in settling particles in the Arabian Sea and its paleogeochemical significance, *Naturwissenschaften, 80*, 511-513, 1993.

Shaffer, G., A model of biogeochemical cycling of phosphorus, nitrogen, oxygen, and sulphur in the ocean: One step toward a global climate model, *J. Geophys. Res., 94 (2)*, 1979-2004, 1989.

Shaffer, G., A non-linear climate oscillator controlled by biogeochemical cycling in the ocean: An alternative model of Quaternary ice age cycles, *Clim. Dyn., 4*, 127-143, 1990.

Smith, S.V., and J.T. Hollibaugh, Coastal metabolism and the oceanic organic carbon balance, *Rev. Geophys. 31*, 75-89, 1993.

Soetaert, K., P.M.J. Herman, and J.J. Middelburg, A model of early diagenetic processes from the shelf to abyssal depths, *Geochim. Cosmochim. Acta, 60*, 1019-1040, 1996a.

Soetaert, K., P.M.J. Herman, and J.J. Middelburg, Dynamic response of deep-sea sediments to seasonal variations: A model, *Limnol. Oceanogr., 41*, in press, 1996b.

Soetaert, K., P.M.J. Herman, J.J. Middelburg, C.H.R. Heip, H.S. de Stigter, T.C.E. van Weering, E. Epping, and W. Helder, Modelling ^{210}Pb-derived mixing activity in ocean margin sediments: Diffusive versus non-local mixing, *J. Mar. Res., 54(6)*, in press, 1996c.

Toggweiler, J.R., and J.L. Sarmiento, Glacial to interglacial changes in atmospheric carbon dioxide: The critical role of ocean surface water in high latitudes, in *The Carbon cycle and Atmospheric CO_2 : Natural Variations Archean to Present, Geophys. Monogr. Ser.*, vol. 32, edited by E.T. Sundquist and W.S. Broecker, pp.163-184, AGU, Washington, D. C. 1984.

Van Cappellen, P., and E. D. Ingall, Benthic phosphorus regeneration, net primary production and ocean anoxia: A model of the coupled marine biogeochemical cycles of carbon and phosphorus, *Paleoceanography, 9(5)*, 677-692, 1994.

Westrich, J. T., and R. A. Berner, The role of sedimentary organic matter in bacterial sulfate reduction: The G-model tested, *Limnol. Oceanogr., 29*, 236-249, 1984.

Wollast R., The coastal organic carbon cycle: Fluxes, sources, and sinks, in *Ocean Margin Processes in Global Change*, edited by R.F.C. Mantoura, J.-M. Martin, and R. Wollast, pp. 365-381, Wiley &, New York, 1991.

C.H.R. Heip, P.M.J. Herman, J.J. Middelburg, and K. Soetaert, Centre for Estuarine and Coastal Ecology, Netherlands Institute of Ecology, Vierstraat 28, 4401 EA Yerseke, Netherlands (e-mail: Heip@cemo.nioo.knaw.nl; Herman@cemo.nioo.knaw.nl; Middelburg @cemo.nioo.knaw.nl; Soetaert@cemo.nioo.knaw.nl)